Active RNA Interference In Mitochondria

Kuanxing Gao[1,2,†], Man Cheng[2,†], Xinxin Zuo[1], Jinzhong Lin[3], Kurt Hoogewijs[4], Michael P. Murphy[5,6], Xiang-Dong Fu[7,*] and Xiaorong Zhang[2,*]

[1]State Key Laboratory of Virology and Hubei Key Laboratory of Cell Homeostasis, College of Life Sciences, Wuhan University, Wuhan, China
[2]Key Laboratory for RNA Biology, Institute of Biophysics, Chinese Academy of Science, Beijing, China
[3]State Key Laboratory of Genetic Engineering, Fudan University, Shanghai, China
[4]Department of organic and macromolecular chemistry, University of Ghent, Ghent, Belgium
[5]Medical Research Council-Mitochondrial Biology Unit, University of Cambridge, Cambridge, UK
[6]Department of Medicine, University of Cambridge, Cambridge, UK
[7]Department of Cellular and Molecular Medicine, Institute of Genomic Medicine, University of California, San Diego, La Jolla, USA

[†] These two authors contributed equally to this work
*To whom correspondence should be addressed. Xiaorong Zhang, email: xrzhang@ibp.ac.cn, or Xiang-Dong Fu, email: xdfu@ucsd.edu

Abstract (Limit: 250 words, currently 172)

RNA interference (RNAi) has been thought to be a gene-silencing pathway present in most eukaryotic cells to safeguard the genome against retrotransposition. Small interfering RNAs (siRNAs) have also become a powerful tool for studying gene functions. Given the endosymbiotic hypothesis for the origin of mitochondria from prokaryotes, mitochondria have been generally assumed to lack active RNAi; however, certain bacteria have Argonaute homologs and various reports suggest the presence of specific microRNAs and nuclear genome (nDNA)-encoded Ago2 in the mitochondria. Here we report that transfected siRNAs are not only able to enter the matrix of mitochondria, but also function there to silence specifically targeted mitochondrial transcripts. The mitoRNAi effect is readily detectable at the mRNA level, but only recordable on relatively unstable proteins, such as the mtDNA-encoded complex IV subunits. We also apply mitoRNAi to directly determine the postulated crosstalk between individual respiratory chain complexes, suggesting that controversy observations previously made on patient-derived cells might result from differential adaptation in different cell lines. Our findings bring a new tool to study mitochondrial biology.

Introduction

Small RNAs, including small interference RNA (siRNA), microRNA (miRNA), and piRNA, play critical roles in regulated gene expression in eukaryotic cells. The RNA interference (RNAi) pathway has been well elucidated in most eukaryotic cells[1-6]. Even lower eukaryotes, such as various yeast, have active RNAi, although certain yeast species, such as budding yeast, have lost such capability, which can be restored by re-expressing specific enzymes in the RNAi pathway[1]. RNAi has been leveraged to study gene functions in diverse biological contexts. Interestingly, however, it has been unclear, even to date, whether an RNAi-like mechanism could operate in the mitochondria, which are thought to originate from parasitic bacteria[7]. The conundrum is that certain bacteria are known to have homologs of Argonaute, a key enzyme in the RNA-Induced Silencing Complex (RISC) responsible for targeted RNA degradation in higher eukaryotic cells[8], and that we and others have demonstrated that specific miRNAs are not only detectable, but also functional in the mitochondria[9,10]. As miRNAs and siRNAs basically utilize the same machineries for their processing and function, the question is whether an RNAi-like mechanism could also function in the mitochondria, and if so, why it has never been reported in literature.

Mitochondria are endosymbiotic organelles in eukaryotic cells, which function as a powerhouse to generate ATP through oxidative phosphorylation (OXPHOS). Interestingly, unlike all living organisms whose genome size is largely proportional to their organismal complexity, the mitochondrial genome becomes minimized during evolution. The human mitochondrial genome, for example, is only of ~16 kb in length and encodes 2 essential rRNAs and a minimal set (22) of tRNAs for translation as well as

13 polypeptides, all of which are membrane proteins as part of the respiratory chain complexes[11]. Essentially all biochemical activities in mitochondria require nuclear genome (nDNA)-encoded proteins[12]. While many nDNA-encoded proteins carry specific signal sequences to enter the mitochondria, at least 30% of them lack such signals[13], and whether certain RNAs can enter mitochondria has been an open, highly debatable question[14,15]. Many lower eukaryotes clearly need import of tRNAs for mitochondrial translation, as some mtDNAs do not even encode any[16] while others miss some key ones[17]. Given the increasing evidence against mitochondrial import of the RNA component of RNase P and 5S rRNA[18,19], the field has been left with a general impression that RNA import into the mitochondria has permanently lost in mammalian cells[20]. The lack of reliable functional readouts for potential RNA import has basically dampened the field towards a resolution to this fundamental question, not mentioning the lack of an effective tool for direct perturbation of mtDNA-encoded genes.

In this study, we sought to systematically investigate whether siRNAs and shRNAs are able to target mtDNA-encoded transcripts. Interestingly, we found that while randomly designed siRNAs do not always show anticipated effects, those following mapped Ago2 binding peaks are all able to specifically target the intended mtDNA-encoded transcripts in an Ago2-dependent manner. We further show that most mitochondrial proteins are remarkably stable, thus preventing the detection of the anticipated RNAi effects at the protein levels, which might explain the lack of report on active mitoRNAi to date. We illustrate the use of this newly established siRNA tool to address some key questions on mitochondrial biology, which has been relied on the limited resource of patient-derived cells. Active mitoRNAi may also serve as an

activity-based platform for future dissection of RNA import mechanism in the mitochondria.

Results

Localization of exogenous small RNAs in mitochondrial matrix

Multiple groups have reported the detection of endogenous small RNAs in the mitochondria[9,21]. To determine whether exogenous small RNAs are able to enter the mitochondria, we transfected a Cy3-labelled siRNA of 21nt into C2C12 cells. We purified mitochondria from transfected cells and showed the enrichment with mitochondrial matrix proteins (i.e. HSP60 and MRPL44), and trypsin treatment removed specific outer membrane (i.e. Tom20) and endoplasmic reticulum (i.e. ERP44) proteins in the absence of Triton-X100 (Fig. 1a). Using highly such purified mitochondria, we performed the nuclease-protection assay with a transfected fluorescent siRNA, which was resistant to treatment with RNase T1 plus Micrococcal Nuclease (MNase) in the absence of Triton-X100 and became sensitive to these nucleases in the presence of the detergent (Fig. 1b). Furthermore, to visualize whether transfected siRNA distributes in mitochondria, we transfected FAM labelled COXI siRNA in OMM-mCherry (TOM20) and su9-BFP (mitochondrial presequence of subunit 9 of the F_0-ATPase which marks mitochondrial matrix) expressed MEF cells. FAM signal located in su9-BFP labeled compartment indicates the distribution of siRNA in mitochondrial matrix (Supplementary information, Fig. S1 and Video S1). These findings provide initial evidence for the ability of exogenous siRNA to localize in mitochondrial matrix.

We next used similarly purified and characterized mitochondria from mouse heart to perform an *in vitro* import assay with a ^{32}P-labled 22nt small RNA, and after RNase treatment to remove outside RNA, we found that a significant fraction of the RNA was readily detectable within the mitochondria (Fig. 1c). In our hands, small RNAs with or without the ability to target a specific mtDNA transcript were both able to import in this assay (data not shown), but a slightly longer RNA of 77nt in length was not (Fig. 1c). These data suggest that small RNA might enter mitochondria through an existing pore(s) on mitochondrial membrane, but unlike ATP-dependent mitochondrial import of tRNAs demonstrated in yeast and other lower eukaryotic organisms[22,23], small RNA import appears to take place in an ATP-independent manner (Fig. 1c). At this point, the nature of such pore or the import mechanism remains a subject of ongoing investigation (see Discussion).

Because the nuclease-resistance assay does not differentiate the localization of imported small RNA in the inter-membrane space versus the matrix of mitochondria, we next sought to determine whether small RNA is able to localize in mitochondrial matrix where siRNA is supposed to function. To this end, we employed a newly developed mitochondrial ClickIn strategy, which utilizes the mitochondria-targeted cyclooctyne (MitoOct) to conjugate any peptide or RNA that carry an azido group (Fig. 1d). As MitoOct is accumulated several hundred-fold within mitochondrial matrix driven by the mitochondrial membrane potential, it will only react with azide-labeled RNA within mitochondrial matrix, as the concentration of MitoOct elsewhere would be too low to drive this reaction[24,25]. Using this strategy, we performed *in vitro* mitochondrial import with an azide-labeled siRNA and then load MitoOct onto the

mitochondria. We found that ~45% of this siRNA reacted with MitoOct within mitochondrial matrix (Fig. 1e). A key control of this assay is to show the dependence of MitoOct loading on the mitochondrial membrane potential, which could be blocked by the uncoupler carbonyl cyanide 4-(trifluoromethoxy) phenylhydrazone (FCCP)[24,25]. We thus first incubated purified mitochondria with RNA, after washing the mitochondria to get rid of extra RNA, we tested the reaction of MitoOct with imported small RNA in the presence or absence of FCCP. As expected, FCCP effectively prevented this reaction (Fig. 1e). These data demonstrate the structural integrity of our purified mitochondria and the ability of small RNA to enter into mitochondrial matrix.

MitoRNAi functions effectively at the RNA level

The ability of a synthetic small RNA to enter mitochondrial matrix prompted us to ask whether such small RNA could elicit RNAi within the mitochondria. We thus prepared siRNAs to target a specific mtDNA-encoded transcript (i.e. ND1). By Northern blotting, we found that some siRNAs showed no effect while others were able to down-regulate the ND1 transcript to a measurable degree (Supplementary information, Fig. S2a). As arbitrarily designed siRNAs did not seem to always work (which might explain early unsuccessful attempts in testing potential RNAi in mitochondria), we reasoned that the failed or inefficient cases might reflect inaccessibility of those siRNAs to targeted mRNA regions. We thus took advantage of mapped Ago2 binding sites generated earlier (by cross-linking immunoprecipitation sequencing or CLIP) in C2C12 cells[9] to design a new set of siRNAs according to Ago2 binding peaks wherever possible (Fig. 2a; all siRNAs listed in Supplementary

information, Table. S1), and observed that the new set of siRNAs each reduced the corresponding mitochondrial transcript as detected by RT-qPCR (Fig. 2b; all primers listed in Supplementary information, Table. S2). We did not observe any specific sequence/motif among these effective siRNAs. To rule out the contribution of pseudogene derived RNA to the observed effect of mitoRNAi, we generated mitochondrial DNA deleted C2C12 cells (ρ^0), then quantified mitochondrial and potential pseudogene derived RNA. The results showed that these barely detectable transcripts were comparable to low-level mtDNA in ρ^0 cells (Fig. 2c). We further validated the siRNA effects by northern blotting in the cases of ND1 and COXI in C2C12 cells (Fig. 2d, e) and ND1 in HeLa cells (Fig. 2f). To get rid of cytosolic RNA contamination, purified mitochondria from COXI, COXII, COXIII, and ATP6 siRNA treated C2C12 cells was analyzed by northern blotting, these results strengthen the effect of siRNA in mitochondria (Fig. 2d and Supplementary information, Fig. S3). We further extended these findings to multiple other cell types (Supplementary information, Fig. S2b, c).

In the cytoplasm, both transfected siRNA and plasmid-expressed small hairpin RNA (shRNA) can elicit RNAi. We tested multiple shRNAs against mtDNA-encoded ND1, COXI, COXII, and COXIII in transfected HEK293T cells and detected recordable, but somewhat variable effects (likely due to different transfection efficiencies), which became enhanced upon selection for the transfected plasmids (Fig. 2g-j). The RNAi effects observed on these individual cell lines also helped to argue against a possibility that transfection reagent might somehow stress the cells to enable transfected siRNA molecules to enter the mitochondria. Collectively, these data strongly suggest that the RNAi pathway operates in the mitochondria.

Ago2-dependent mitoRNAi

To demonstrate the targeting specificity of transfected siRNAs, we showed that siND1 targeted ND1, but not COXI, and siCOXI reduced COXI, but not ND1 in two different mouse cell types (Fig. 3a). To further validate the specificity, we compared the effects of mutations (from position 9 to 13) in wild-type (WT) siCOX1 and siND1 (Fig. 3b) and found that both mutant siRNAs lost the effect on their targeted mRNAs (Fig. 3c). This is consistent with the known base-paring requirement within the mRNA:siRNA duplex for the siRNA effect in the cytoplasm[26].

The RNAi pathway is known to function via the RISC complex in the cytoplasm. In mammalian cells, argonaute-2 (Ago2), which is the only catalytically active Argonaute[8], is able to elicit the siRNA effect through its slicing activity. Using the standard curve generated with purified Ago2 protein, we quantified endogenous Ago2 protein level in purified mitochondria and whole cell. The result indicated that about 5% of Ago2 localize in mitochondria (Supplementary information, Fig. S4a). Furthermore, overexpressing mitochondria-targeted Ago2 into MEF cells enhanced the effect of mitoRNAi at RNA level, but not protein level (Supplementary information, Fig. S4b). To determine the functional requirement of Ago2 for the newly observed RNAi activity, we tested a pair of WT and Ago2 knockout (KO) mouse embryonic fibroblast (MEF) lines. As expected, both siND1 and siCOXI down regulated their targets in WT, but not in Ago2 KO MEFs (Fig. 3d, e). The RNAi effects could be fully rescued by expressing WT Ago2, which can function in both cytoplasm and mitochondria (Supplementary information, Fig. 4c). To avoid potential compound

effects due to some unknown crosstalk between the cytoplasm and the mitochondria, we tested and showed the rescue with a mitochondria-targeted WT Ago2 (su9-Ago2), and importantly, the slicing defective mutant su9-Ago2 (D597A) failed to rescue in both siND1 and siCOXI-treated cells (Fig. 3d, e). Together, these data established Ago2 slicing activity-dependent mitoRNAi.

Impact of mitoRNAi on mtDNA-encoded proteins

We initially intended to demonstrate the RNAi effect at the protein levels, but in most cases, we saw little impact, which might have discouraged early efforts in assessing potential mitoRNAi. We reasoned that mtDNA-encoded proteins might be too long-lived to detect the RNAi effect within the standard window (2 to 3 days) normally used for targeting nDNA-encoded gene products. To test this possibility, we analyzed the protein levels of multiple subunits of OXPHOS complexes at different time points after blocking mitochondrial translation with chloramphenicol (INN)[27]. We found that representative components of OXPHOS complexes I, II, III and V all showed little change in the absence of mitochondrial translation for up to 48 hours in MEF cells (Fig. 4a; all antibodies listed in Supplementary information, Table. S3) and we made similar observation on C2C12 cells (Supplementary information, Fig. S5a). The only exception is complex IV in which all three mtDNA-encoded components (COXI, II, and III) and representative nDNA-encoded subunits (e.g. COX5B) were significantly reduced in 24 hours after INN treatment (Fig. 4a). Corroborating these observations, the siRNAs against COXI, II, and III diminished their targets at both RNA (Supplementary

information, Fig. S5b) and protein levels (Fig. 4b) in C2C12 cells. In contrast, siND1 showed little effect in reducing ND1 protein (Fig. 4c).

We reasoned that if mitoRNAi were masked on most mtDNA-encoded proteins, compromised protein stability would enable us to detect such effects. We therefore tested knockdown of an nDNA-encoded complex I component NDUFA13, which is known to destabilize this complex[28], and indeed, we were able to record the enhanced siND1 effect to a measurable degree (Fig. 4c). Furthermore, to test whether the other relative stable complex subunit can be downregulated by siRNA, we extended siRNA treatment against ND1 (CXI), CytB (CXIII), and ATP6 (CXV) from 48 hours to 72 hours, and the results showed that these protein level decreased at 72 hours (Supplementary information, Fig. 5c). Because transcription and translation are coupled in mitochondria[29-31], we predicted that reduced mRNA would directly decrease the rate of nascent protein synthesis on mitochondrial ribosomes. To test this, we performed ^{35}S-labeling experiments in the presence of Emetine to block cytoplasmic translation in C2C12 cells. As expected, COXI nascent protein synthesis was markedly reduced in response to siCOXI treatment while translation of all other mitochondrial transcripts was unaltered (Fig. 4d). Collectively, these data provide strong evidence for active mitoRNAi, which likely escaped previous detection because of remarkable stability of most mtDNA-encoded proteins.

Using mitoRNAi to test communication among respiratory chain complexes

The establishment of active mitoRNAi afforded us a new tool to directly address some fundamental questions on mitochondrial biology, which have been mainly studied through manipulating nDNA-encoded subunits/assembly factors or by analyzing

mutations in mtDNA-encoded genes identified in patients[32]. To illustrate the power of this newly enabled technology, we focused on addressing potential crosstalk between different respiratory chain complexes, as various contradictory results have been reported in literature. The OXPHOS complex is composed of five complexes (I, II, III, IV, and V), and except complex II (which is only composed of nDNA-encoded subunits), all contain both nDNA- and mtDNA-encoded subunits. Complex I, III, and IV are further assembled into various supercomplexes, and to date, the assembly of complex II has been thought to be largely independent of all other OXPHOS complexes[33-35]. In contrast, mutations in mtDNA-encoded complex IV subunits have been reported to affect only complex IV[36], compromise both complex I and IV[37], or all OXPHOS respiratory chain complexes[38,39]. Because these reports were all based on analysis of patient-derived cell lines, it remains unclear whether the discrepancies resulted from direct impact of different mutations and/or differential adaptation of those patient-derived cells after long-term culture *in vitro*.

To address these possibilities, we took advantage of the newly developed siRNA tool to transiently knock down COXI, II or III in C2C12 cells, all leading to compromised oxygen consumption, similar to that induced by down-regulating nDNA-encoded COX4, as indicated by the dramatic reduction of the maximal respiratory capacity (Fig. 5a). As expected, knockdown of either COXI or COX4 reduced mitochondrial membrane potential as measured by accumulated tetramethyl-rhodamine methyl ester (TMRM) fluorescence dye (Fig. 5b). These data corroborated the selective decrease of complex IV assembly, as revealed by blue native gel electrophoresis (BN-PAGE) (Fig. 5c) and in-gel activity assay (Fig. 5d). Using these assays, we next

examined the impact of compromised complex IV on the assembly/stability of other OXPHOS complexes. We found little impact on complex I, III and V, and we did not detect any effect of nDNA-encoded COX4 either on the complexes (Fig. 5e). These findings favor the possibility that the postulated influence of complex IV on the stability/assembly of complex I[37] or all other respiratory chain complexes[38,39] likely resulted from adaptation of patient-derived cells. Unexpectedly, we detected an increase in complex II (Fig. 5e). We suspect that compromised complex IV might reduce efficient electron transfer along the respiratory chain, thus causing a selective "damping" effect to account for increased complex II.

Discussion

The reason why mitoRNAi might have escaped early detection is likely due to (i) the theoretical consideration of the bacterial origin of the mitochondria, (ii) blockage of siRNA accessibility to many mRNA regions because mitochondrial transcription and translation both take place on inner membrane, and (iii) remarkably stability of most mtDNA-encoded proteins. By experimentally addressing the latter two obstacles, we now demonstrate active RNAi in the mitochondria. Our findings are in line with our previous report of miRNA function in the mitochondria[9]. Interestingly, imperfect base-pairing between a specific miRNA and its mtDNA-encoded transcript leads to enhanced translation whereas perfect base-pairing between a specific siRNA and its target triggers mRNA degradation. While both of these reactions require Ago2, the siRNA function, but not that of miRNA, depends on the slicing activity of Ago2.

An unsolved question is how siRNA and miRNA may translocate to the matrix of mitochondria. During this investigation, we have made elaborated efforts in exploring potential mechanism(s) for small RNA import into mitochondria, including targeting various molecules previously implicated in RNA import into mitochondria, such as PNPT1[40], GRSF1[41], and TOM complex[42]. We also tested blockage of mitochondrial outer membrane permeability (MOMP) and the permeability transition pore (MPTP)[43,44]. So far, we have not yet obtained any convincing data. Of note, a recent report suggests exporting mitochondrial RNA to induce innate immunity in mammalian cells[45], but the mechanism has also remained elusive. Therefore, future studies are clearly required to elucidate the mechanism for RNA import to or export out of mitochondria. We suggest that active mitoRNAi may serve a functional readout for future investigation of this fundamental problem.

Despite unclear mechanism for small RNA to enter mitochondria, the established activities of both siRNA and miRNA within the mitochondria would provide very useful tools to directly modulate the function of mtDNA-encoded genes, which has been solely relied on patient-derived cells. It is interesting to note that miRNA-enhanced mitochondrial translation has been linked to a role of miR-21 in lowing blood pressure in a rat spontaneous hypertension model[46]. The newly demonstrated mitoRNAi points to a potential therapeutic intervention strategy against human diseases caused by mutations in the mitochondrial genome. For example, this precision RNA cleavage tool may be used to selectively remove mutated mitochondrial transcripts, which often co-exist with wild-type transcripts in patients heteroplasmic for mtDNA mutations. Thus, the

newly established mitoRNAi is expected to drive both basic and clinical research on mitochondrial biology.

Materials and Methods

Cell culture and transfection

C2C12, LLC, MEF, 4T1, HeLa, and 293T cells were all cultured in Dulbecco's Minimal Essential Medium (DMEM, Life Technology) supplemented with 10% fetal bovine serum (Life Technology). Cells were maintained in 5% CO_2 at 37^{o}C. For transfection with siRNA, Lipofectamine RNAiMAX (Invitrogen) was used according to manufacturer's instruction. After siRNA treatment for 48 hrs, cells were collected with Trizol (Invitrogen) for RNA analysis by RT-qPCR and northern blotting or with SDS-loading buffer for protein analysis by Western blotting.

Generation of shRNA expressing stable cell lines

Synthetic shRNA oligonucleotides were inserted into the pLKO.1 plasmid between Age I and EcoR I sites. The plasmid was co-transfected with psPAX2 and pMD2G at the ratio 5: 3.75: 1.25 into HEK293T cells to produce lentivirus in 6 cm dish. Collected lentivirus was used to infect HEK293T for 24 hours followed by selection against puromycin (Sigma) at the concentration of 2 ng/ml for 6 days.

Mitochondria isolation

Mouse heart or cells were homogenized with isolation buffer (250 mM Sucrose, 10 mM Tris-HCl pH7.4, 1 mM EDTA) by Dounce (Sigma), as described earlier [47]. The

homogenate was next separated with the following steps: first, clear cell debris at 800g twice and then at 1200g twice in 4^{o}C for 5 min; second, transfer the supernatant to a new tube and pellet crude mitochondria at 15000g for 10 min; third, resuspend the crude mitochondria pellet with isolation buffer and lay it on a sucrose gradient (17%, 31%, 42%, 50%) prepared with $T_{10}E_{20}$ buffer (10mM Tris-HCl, pH7.4 and 20mM EDTA-Tris, pH7.4), as previously described[9]. The sucrose gradient with crude mitochondria was centrifuged in SW41 rotor (Beckman) at 18000rpm for 45 min. Mitochondria were collected at the layer between 42% and 50% sucrose.

Small RNA importing assay

To assay for small RNA import *in vitro*, mitochondria isolated from mouse heart were divided into five aliquots. Individual aliquots were incubated with 77nt ^{32}P-labelled RNA or 22nt Cy3-labeled RNA at 37 ^{o}C for 30min. Two of these aliquots were also added with ATP (2 mM). After incubation, the rest of aliquots except the input aliquot were subject to RNase T1 (3000U/ml, Thermo Scientific) digestion on ice for 30 min. Mitochondria were pelleted by centrifugation and RNA extracted with Trizol. RNA in aliquots incubated with 77nt ^{32}P-labeled RNA were resolved in a 12% urea-page gel whereas RNA in aliquots incubated with 22nt Cy3-labeled RNA were resolved in a 15% urea-page gel. The gels were scanned on a typhoon instrument (GE) for quantification.

To assay for small RNA import *in vivo,* mitochondria isolated from C2C12 cells transfected with 22nt Cy3-labeled siRNA were divided into three aliquots with one aliquot standing on ice as control, and the other two aliquots were subjected to

digestion with RNase T1 (3000U/ml) plus Micrococcal nuclease (1000U/ml) on ice for 30 min in the presence or absence of Triton X-100, as described earlier [9]. Total lysate served as control. Mitochondria were pelleted by centrifugation at 20000g and RNA extracted with Trizol for analysis by RT-qPCR. 7SK, 16S rRNA, and GAPDH RNAs served as internal controls.

Click-In chemistry assay

The Click-In chemistry assay was performed as reported [24]. Briefly, purified mitochondria from mouse heart were divided into 3 aliquots and all incubated with ^{32}P-labeled and azido-tagged siRNA in KCl buffer (120 mM KCl, 10 mM HEPES-KOH, 1mM EGTA, 1mM ADP, 1mM $MgCl_2$, 1mM KPi, 0.05% BSA, pH7.4 supplemented with 10 mM potassium succinate) for 1 hour. Free RNA was removed by washing with STE buffer (250 mM sucrose, 5 mM Tris, 1 mM EGTA, pH 7.4) for 3 times. MitoOCT was added in the presence or absence of FCCP and incubated at 37 ^{o}C for 1 hour. After incubation, mitochondria were pelleted at 12000g for 2 min, and after washing with STE buffer, the pellet was resuspended in 50 µl SET buffer. RNase T1 and Tetrazine were added at the final concentrations of 3000 U/ml and 50 µM, respectively, on ice for 20 min. Mitochondria were pelleted by centrifugation at 20000g and RNA extracted with Trizol for downstream analysis. RNA-azide-OCT could be readily separated from unreacted RNA-azide in 20% urea denaturing gel. The gel was exposed to a phosphor imager overnight and scanned in a Typhoon Scanner (GE).

Northern blotting and RT-qPCR

For Northern blotting, C2C12 or HeLa cells were first transfected with siRNA for 48 hours and RNA extracted with Trizol. 10μg RNA was separated on 1.5% formaldehyde agarose gel and blotted with probes (listed in Supplementary information, Table. S2). For Northern blotting analysis of COXI RNA after siRNA treatment, mitochondria were first purified before RNA extraction. For RT-qPCR, RNA was extracted with Trizol 48 hours after siRNA transfection. cDNA was synthesized by reverse-transcription (M-MLV, Promega) with random primers (N9). cDNA was quantified with Master SYBR Green Mix (Roche) on Bio-Rad Touch FX96.

Analysis of mitochondrial protein stability

MEFs or C2C12 cells were first plated on 6-well plate with 10% FBS DMEM, and after reaching 70%-80% confluency, the culture medium was replaced with 10% FBS DMEM containing 250 μg/ml (for MEFs) or 150 μg/ml (for C2C12 cells) chloramphenicol. Samples were collected from 0 to 48 hours at 12 hours intervals. All samples were lysed with SDS-loading buffer and analyzed by Western blot with different antibodies (Listed in Supplementary information, Table. S3).

Mitochondrial translation assay

^{35}S-Cys/Met was used to label nascent peptides according to the procedure [48]. C2C12 cells were first transfected with siRNA on 6-well plate and culture medium was replaced with labeling medium (cysteine and methionine-free DMEM

supplemented with 10% dialyzed FBS) for 30 min at 37^{o}C. Emetine (100 μg/ml) was added to the labeling medium for 5 min. EasyTag ^{35}S-labeling mixture (PerkinElmer) was added to the labeling medium to final 200 μCi/ml and the reaction was incubated for 1 hour. Labeled proteins were collected with SDS-loading buffer and resolved in 17.5% SDS-PAGE. After the electrophoresis, the gel was dried and exposed to phosphor screen for 2 days and analyzed on a Typhoon scanner (GE).

BN-PAGE and in-gel activity

Mitochondrial respiratory complex and activity were analyzed with blue native-page (BN-PAGE) and in gel activity assay, respectively. The procedure of BN-PAGE was as previously described[49]. Briefly, C2C12 cells were first transfected with siRNA and plated on 60 mm dish. After cell confluency reaching 90% in about 48 hours, cells were transferred to a 1.5 ml tube and washed once with ice-cold PBS. Cells were pelleted and protein concentration analyzed with BCA (Pierce). The cell pellet was re-suspended with a volume (X) of ice-cold PBS to final concentration of 5 mg/ml. An equal volume of digitonin (4 mg/ml) was added and the reaction was incubated on ice for 10min. The pellet was washed three times with pre-cold PBS to remove residual digitonin and then re-suspended with BN sample buffer (half volume of X) and 10% DDM (one-tenth volume of X) and then incubated on ice for 20 min. Sample was cleared by centrifugation at 20000g for 20 min and the supernatant transferred to a fresh tube containing 5% SBG (half volume of 10% LM used). BN samples were separated on 3%-15% blue native gel. Antibodies were used to probe the complex

abundance (Listed in Supplementary information, Table. S3). Reagents used to detect complex I and complex IV activities were as described[50].

Measurement of mitochondrial oxygen consumption rate and membrane potential

Mitochondrial oxygen consumption rate was measured on Seahorse as described[51]. C2C12 cells were first transfected with siRNA in 12-well plate. After cell confluency reaching 90% in 48 hours, about 30000 cells were replated on a 24-well Seahorse plate. Cells were refreshed with detection solution gradually to the final volume of 525 µl and incubated at 37 ^{o}C for 1 hour. Cells were configured with a mito stress kit and probe plate pretreated with XF Celebrant pH-7.4 at 37 ^{o}C according to manufacturer's instruction. The samples were analyzed with Seahorse XF24 software on Seahorse XF24 Extracellular Flux Analyzer (Seahorse Bioscience).

Mitochondrial membrane potential was measured by FACS, as described[52]. C2C12 cells were first transfected with siRNA and seeded on 6-well plate. Trypsinized cells were resuspended in DMEM and washed twice with pre-cold PBS. Cells were stained with 100 µl 100 nM TMRM (Invitrogen) in DMEM without phenol and incubated at 37 ^{o}C for 30 min. Stained cells were washed twice with pre-cold PBS and detected by FACS on the exciting wavelength 488 and emission wavelength 570nm. Data were analyzed with FlowJo.

Immunocytochemistry

Fam conjugated COXI siRNAs were transfected into TOM20-mCherry (outer membrane) and subunit 9 of ATP synthase (su9)-BFP (matrix) expressed MEF cells. After 5hrs transfection, cells were washed with PBS 5-10 times and analyzed with

Structured Illumination Microscopy (SIM) (Delta Vision OMX). The signals captured by SIM were reconfigured with the Softworx 6.0 Beta 19. Then the 3D image was processed with Imaris. The FAM-siCOXI signal in mitochondria was extracted and the signal outside of mitochondria was discarded. The picture and movie were all produced by Imaris.

Acknowledgments

This work was supported by grants from the Ministry of Science and Technology of China (2017YFA0504600, 2019YFA0508700 and 2017YFA0504400), the National Natural Science Foundation of China (31670825 and 91440102), and Chinese Academy of Science foundation grant (22KJZD-EW-L12) to X.Z. Work in the Murphy lab was supported by the Medical Research Council UK (MC_U105663142) and by a Wellcome Trust Investigator award (110159/Z/15/Z). We also acknowledge the contribution of Drs. Yi Zhang and Yuanchao Xue in the early phase of this project, Dr. Heping Cheng for providing the Seahorse apparatus, and Hongjie Zhang for isotope experiment assistance. We are grateful to Drs. Immo Scheffler, Jing Hu and Peter Rehling for critical comments on the manuscript.

Author Contributions

X.Z. and X-D.F. designed the experiments; K.G., M.C., and X.Z. performed most experiments; X-X.Z. helped with data analysis; J.L. contributed to experimental design and data interpretation; M.P.M. and K.H. designed the Click-In experiment and provided the MitoOct reagents; X.Z., K.G and X-D.F. wrote the paper and M.P.M. and K.H. revised the paper.

Conflict of interest

The authors declare that they have no conflict of interest.

References

1 Drinnenberg, I. A. et al. RNAi in budding yeast. Science 326, 544-550, doi:10.1126/science.1176945 (2009).

2 Fire, A. et al. Potent and specific genetic interference by double-stranded RNA in Caenorhabditis elegans. Nature 391, 806-811, doi:10.1038/35888 (1998).

3 Hamilton, A. J. & Baulcombe, D. C. A species of small antisense RNA in posttranscriptional gene silencing in plants. Science (New York, N.Y.) 286, 950-952 (1999).

4 Imig, J. et al. miR-CLIP capture of a miRNA targetome uncovers a lincRNA H19-miR-106a interaction. Nature chemical biology 11, 107-114, doi:10.1038/nchembio.1713 (2015).

5 Elbashir, S. M. et al. Duplexes of 21-nucleotide RNAs mediate RNA interference in cultured mammalian cells. Nature 411, 494-498, doi:10.1038/35078107 (2001).

6 Shi, Y. Mammalian RNAi for the masses. Trends in Genetics 19, 9-12, doi:https://doi.org/10.1016/S0168-9525(02)00005-7 (2003).

7 Roger, A. J., Munoz-Gomez, S. A. & Kamikawa, R. The Origin and Diversification of Mitochondria. Current biology : CB 27, R1177-r1192, doi:10.1016/j.cub.2017.09.015 (2017).

8 Liu, J. et al. Argonaute2 is the catalytic engine of mammalian RNAi. Science (New York, N.Y.) 305, 1437-1441, doi:10.1126/science.1102513 (2004).

9 Zhang, X. R. et al. MicroRNA Directly Enhances Mitochondrial Translation during Muscle Differentiation. Cell 158, 607-619, doi:10.1016/j.cell.2014.05.047 (2014).

10 Kren, B. T. et al. MicroRNAs identified in highly purified liver-derived mitochondria may play a role in apoptosis. RNA biology 6, 65-72 (2009).

11 Koopman, W. J. H., Distelmaier, F., Smeitink, J. A. M. & Willems, P. H. G. M. OXPHOS mutations and neurodegeneration. Embo Journal 32, 9-29, doi:10.1038/emboj.2012.300 (2013).

12 Ojala, D., Montoya, J. & Attardi, G. tRNA punctuation model of RNA processing in human mitochondria. Nature 290, 470-474 (1981).

13 Moulin, C., Caumont-Sarcos, A. & Ieva, R. Mitochondrial presequence import: Multiple regulatory knobs fine-tune mitochondrial biogenesis and homeostasis. Biochim Biophys Acta Mol Cell Res 1866, 930-944, doi:10.1016/j.bbamcr.2019.02.012 (2019).

14 Jeandard, D. et al. Import of Non-Coding RNAs into Human Mitochondria: A Critical Review and Emerging Approaches. Cells 8, doi:10.3390/cells8030286 (2019).

15 Isaac, R. S., McShane, E. & Churchman, L. S. The Multiple Levels of Mitonuclear Coregulation. Annual review of genetics 52, 511-533, doi:10.1146/annurev-genet-120417-031709 (2018).
16 Schneider, A. Unique aspects of mitochondrial biogenesis in trypanosomatids. Int J Parasitol 31, 1403-1415, doi:10.1016/s0020-7519(01)00296-x (2001).
17 Schneider, A. Mitochondrial tRNA import and its consequences for mitochondrial translation. Annu Rev Biochem 80, 1033-1053, doi:10.1146/annurev-biochem-060109-092838 (2011).
18 Holzmann, J. et al. RNase P without RNA: identification and functional reconstitution of the human mitochondrial tRNA processing enzyme. Cell 135, 462-474, doi:10.1016/j.cell.2008.09.013 (2008).
19 Brown, A. et al. Structure of the large ribosomal subunit from human mitochondria. Science 346, 718-722, doi:10.1126/science.1258026 (2014).
20 Kiss, T. & Filipowicz, W. Evidence against a mitochondrial location of the 7-2/MRP RNA in mammalian cells. Cell 70, 11-16, doi:10.1016/0092-8674(92)90528-k (1992).
21 Das, S. et al. Nuclear miRNA regulates the mitochondrial genome in the heart. Circulation research 110, 1596-1603, doi:10.1161/circresaha.112.267732 (2012).
22 Mahapatra, S., Ghosh, T. & Adhya, S. Import of small RNAs into Leishmania mitochondria in vitro. Nucleic acids research 22, 3381-3386 (1994).
23 Rubio, M. A. et al. Mammalian mitochondria have the innate ability to import tRNAs by a mechanism distinct from protein import. Proc Natl Acad Sci U S A 105, 9186-9191, doi:10.1073/pnas.0804283105 (2008).
24 Hoogewijs, K. et al. ClickIn: a flexible protocol for quantifying mitochondrial uptake of nucleobase derivatives. Interface focus 7, 20160117, doi:10.1098/rsfs.2016.0117 (2017).
25 Logan, A. et al. Assessing the Mitochondrial Membrane Potential in Cells and In Vivo using Targeted Click Chemistry and Mass Spectrometry. Cell Metabolism 23, 379-385, doi:10.1016/j.cmet.2015.11.014 (2016).
26 Wang, Y. et al. Structure of an argonaute silencing complex with a seed-containing guide DNA and target RNA duplex. Nature 456, 921-926, doi:10.1038/nature07666 (2008).
27 McKee, E. E., Ferguson, M., Bentley, A. T. & Marks, T. A. Inhibition of mammalian mitochondrial protein synthesis by oxazolidinones. Antimicrobial agents and chemotherapy 50, 2042-2049, doi:10.1128/aac.01411-05 (2006).
28 Stroud, D. A. et al. Accessory subunits are integral for assembly and function of human mitochondrial complex I. Nature 538, 123-126, doi:10.1038/nature19754 (2016).
29 Kehrein, K. et al. Organization of Mitochondrial Gene Expression in Two Distinct Ribosome-Containing Assemblies. Cell reports, doi:10.1016/j.celrep.2015.01.012 (2015).
30 Bogenhagen, D. F., Martin, D. W. & Koller, A. Initial Steps in RNA Processing and Ribosome Assembly Occur at Mitochondrial DNA Nucleoids. Cell Metab. 19, 618-629, doi:10.1016/j.cmet.2014.03.013 (2014).

31 Rackham, O. et al. Hierarchical RNA Processing Is Required for Mitochondrial Ribosome Assembly. Cell reports, doi:10.1016/j.celrep.2016.07.031 (2016).
32 Taylor, R. W. & Turnbull, D. M. Mitochondrial DNA mutations in human disease. Nature reviews. Genetics 6, 389-402, doi:10.1038/nrg1606 (2005).
33 Gu, J. et al. The architecture of the mammalian respirasome. Nature 537, 639-643, doi:10.1038/nature19359 (2016).
34 Wu, M., Gu, J., Guo, R., Huang, Y. & Yang, M. Structure of Mammalian Respiratory Supercomplex I1III2IV1. Cell 167, 1598-1609.e1510, doi:10.1016/j.cell.2016.11.012 (2016).
35 Guo, R., Zong, S., Wu, M., Gu, J. & Yang, M. Architecture of Human Mitochondrial Respiratory Megacomplex I2III2IV2. Cell 170, 1247-1257.e1212, doi:10.1016/j.cell.2017.07.050 (2017).
36 Tiranti, V. et al. A novel frameshift mutation of the mtDNA COIII gene leads to impaired assembly of cytochrome c oxidase in a patient affected by Leigh-like syndrome. Human molecular genetics 9, 2733-2742 (2000).
37 Li, Y. et al. An assembled complex IV maintains the stability and activity of complex I in mammalian mitochondria. The Journal of biological chemistry 282, 17557-17562, doi:10.1074/jbc.M701056200 (2007).
38 Rahman, S. et al. A missense mutation of cytochrome oxidase subunit II causes defective assembly and myopathy. Am J Hum Genet 65, 1030-1039, doi:10.1086/302590 (1999).
39 Hornig-Do, H. T. et al. Nonsense mutations in the COX1 subunit impair the stability of respiratory chain complexes rather than their assembly. The EMBO journal 31, 1293-1307, doi:10.1038/emboj.2011.477 (2012).
40 Wang, G. et al. PNPASE regulates RNA import into mitochondria. Cell 142, 456-467, doi:10.1016/j.cell.2010.06.035 (2010).
41 Noh, J. H. et al. HuR and GRSF1 modulate the nuclear export and mitochondrial localization of the lncRNA RMRP. Genes Dev 30, 1224-1239, doi:10.1101/gad.276022.115 (2016).
42 Wiedemann, N. & Pfanner, N. Mitochondrial Machineries for Protein Import and Assembly. Annu Rev Biochem 86, 685-714, doi:10.1146/annurev-biochem-060815-014352 (2017).
43 Schinzel, A. C. et al. Cyclophilin D is a component of mitochondrial permeability transition and mediates neuronal cell death after focal cerebral ischemia. Proceedings of the National Academy of Sciences of the United States of America 102, 12005-12010, doi:10.1073/pnas.0505294102 (2005).
44 Halestrap, A. P. What is the mitochondrial permeability transition pore? J Mol Cell Cardiol 46, 821-831, doi:10.1016/j.yjmcc.2009.02.021 (2009).
45 Dhir, A. et al. Mitochondrial double-stranded RNA triggers antiviral signalling in humans. Nature 560, 238-242, doi:10.1038/s41586-018-0363-0 (2018).
46 Li, H. et al. MicroRNA-21 Lowers Blood Pressure in Spontaneous Hypertensive Rats by Upregulating Mitochondrial Translation. Circulation 134, 734-751, doi:10.1161/circulationaha.116.023926 (2016).

47 Frezza, C., Cipolat, S. & Scorrano, L. Organelle isolation: functional mitochondria from mouse liver, muscle and cultured fibroblasts. Nature protocols 2, 287-295, doi:10.1038/nprot.2006.478 (2007).
48 Sasarman, F. & Shoubridge, E. A. Radioactive labeling of mitochondrial translation products in cultured cells. Methods in molecular biology (Clifton, N.J.) 837, 207-217, doi:10.1007/978-1-61779-504-6_14 (2012).
49 Leary, S. C. Blue native polyacrylamide gel electrophoresis: a powerful diagnostic tool for the detection of assembly defects in the enzyme complexes of oxidative phosphorylation. Methods in molecular biology (Clifton, N.J.) 837, 195-206, doi:10.1007/978-1-61779-504-6_13 (2012).
50 Khvorostov, I., Zhang, J. & Teitell, M. Probing for mitochondrial complex activity in human embryonic stem cells. Journal of visualized experiments : JoVE, doi:10.3791/724 (2008).
51 Gao, Y. et al. Mammalian elongation factor 4 regulates mitochondrial translation essential for spermatogenesis. Nat Struct Mol Biol 23, 441-449, doi:10.1038/nsmb.3206 (2016).
52 Khacho, M. et al. Mitochondrial Dynamics Impacts Stem Cell Identity and Fate Decisions by Regulating a Nuclear Transcriptional Program. Cell Stem Cell 19, 232-247, doi:10.1016/j.stem.2016.04.015 (2016).

Figures legends

Figure 1. Detection of small RNAs in mitochondria by nuclease Protection, *in vitro* RNA import, and ClickIn. a, The purity of isolated mitochondria analyzed by Western blot for HSP60 and MRPL44 (mitochondrial matrix proteins), Tom20 (mitochondrial outer membrane protein), and ERP44 (endoplasmic reticulum protein). **b**, The distribution of Cy3-labeled siRNA 4 hours after transfection into C2C12 cells and purified mitochondria were subjected to the nuclease protection assay with RNase T1 plus MNase. RNA were resolved by urea or agarose gel and developed by Typhoon scanning or EtBr staining. **c**, ^{32}P-labeled RNA of indicated length were analyzed after incubation with purified mouse heart mitochondria and analyzed by the nuclease protection assay. T1, RNase T1; MN, Micrococcal Nuclease, MT, mitochondria. **d**, Scheme of the ClickIn assay. MitoOct carries a PPh_3 group with high affinity to mitochondrial matrix and a cyclooctyne (Oct) group reactive to azide. FCCP, Carbonyl cyanide-trifluoromethox-phenylhydrazone (FCCP), Tet, tetrazine. **e**, Mitochondria purified from mouse heart were incubated with ^{32}P-labeled and azide-labeled siCOXI followed by the addition of MitoOct in the presence or absence of FCCP. The upper band indicates the MitoOct-modified siRNA in mitochondrial matrix.

Figure 2. Specific targeting of mtDNA-encoded transcripts by siRNA and shRNA. a, siRNAs designed to target individual mtDNA-encoded transcript according to previously mapped Ago2 binding peaks in C2C12 cells. **b**, RT-qPCR analysis of all 13 mitochondrial transcripts in C2C12 cells after treatment with corresponding siRNAs. **c**, qPCR analysis of mtDNA copy number in ρ^0 and WT C2C12 cells (left panel), RT-qPCR analysis of transcripts in ρ^0 and WT C2C12 cells (right panel). **d-f**, Detection of mouse ND1 and COXI mRNAs (c, d) in C2C12 cells and human ND1 mRNAs (e) in HeLa cells by Northern blotting (NB) treated with either control or specific siRNA. rRNAs served as loading control and detected by Northern blotting or direct SYBR^{TM} Gold staining in the same gel. **g-j**, RT-qPCR analysis of COXI, II, III, and ND1 RNA levels in HEK293T cells transient (Trans.) and stable (Infect.) treatment with shCOXI, II, III, and ND1. Data represent average ± SEM based on 3 independent experiments. ***, $p<0.005$, ****, $p<0.001$ based on unpaired Student's t test.

Figure 3. Ago2-dependent mitoRNAi. a, RT-qPCR analysis of ND1 or COXI in 4T1 (up panel) and LLC (lower panel) mouse cells treated with siND1 or siCOXI. **b**, Mutations in siCOXI and siND1 (blue) relative to WT siRNAs (red). **c**, RT-qPCR analysis of COXI or ND1 RNA in C2C12 cells treated with corresponding WT and mutant siRNAs. **d-e**, WT and Ago2 KO MEFs transfected with siND1(d) or siCOXI (e). The RNAi effects were examined in Ago2 KO MEFs complemented with either a mitochondria-targeted Ago2 (su9-Ago2) or its catalytically dead D597A mutant.

Figure 4. Protein stability and siRNA targeting efficiency at protein levels. a, Time-course analysis of representative nDNA- and mtDNA-encoded mitochondrial proteins by

Western blotting in MEF cells after treatment with chloramphenicol (INN). HSP60 and β-actin served as loading control. **b**, Western blotting analysis of COXI, COXII, or COXIII proteins after control (Ctl) or specific siRNA treatment. **c**, Western blot analysis of ND1 protein after treatment with indicated siRNAs. **d.** Mitochondrial translation products were pulse-labeled for 1 hour in C2C12 cells treated with control or COXI siRNA for 48 hours. Coomassie blue-stained gels were used to verify even loading (right panel).

Figure 5. Functional impact after down-regulating complex IV subunits. a, Oxygen consumption rate (OCR) measured in C2C12 cells treated with the indicated siRNAs. COX4 served as a positive control. Oligo: Oligomycin; FCCP, Carbonyl cyanide-trifluoromethox-phenylhydrazone (FCCP); AA&R: Antimycin A plus Rotenone. **b**, Membrane potential measured with Tetramethylrhodamine methyl ester (TMRM) fluorescence in C2C12 cells treated with the indicated siRNAs. **c**, Mitochondria were solubilized with DDM and analyzed by BN-PAGE and immunoblotting. Quantified data were shown in the lower panel. **d**, Mitochondria were solubilized and analyzed by BN-PAGE followed by in-gel activity assay for complex I (top) or complex IV (bottom). **e**, BN-PAGE and immunoblotting analysis of individual mitochondrial complexes (labeled on top in each panel) with antibodies after treatment with the indicated siRNAs. The statistics shown on the right was based on 3 independent biological replicates in each case.

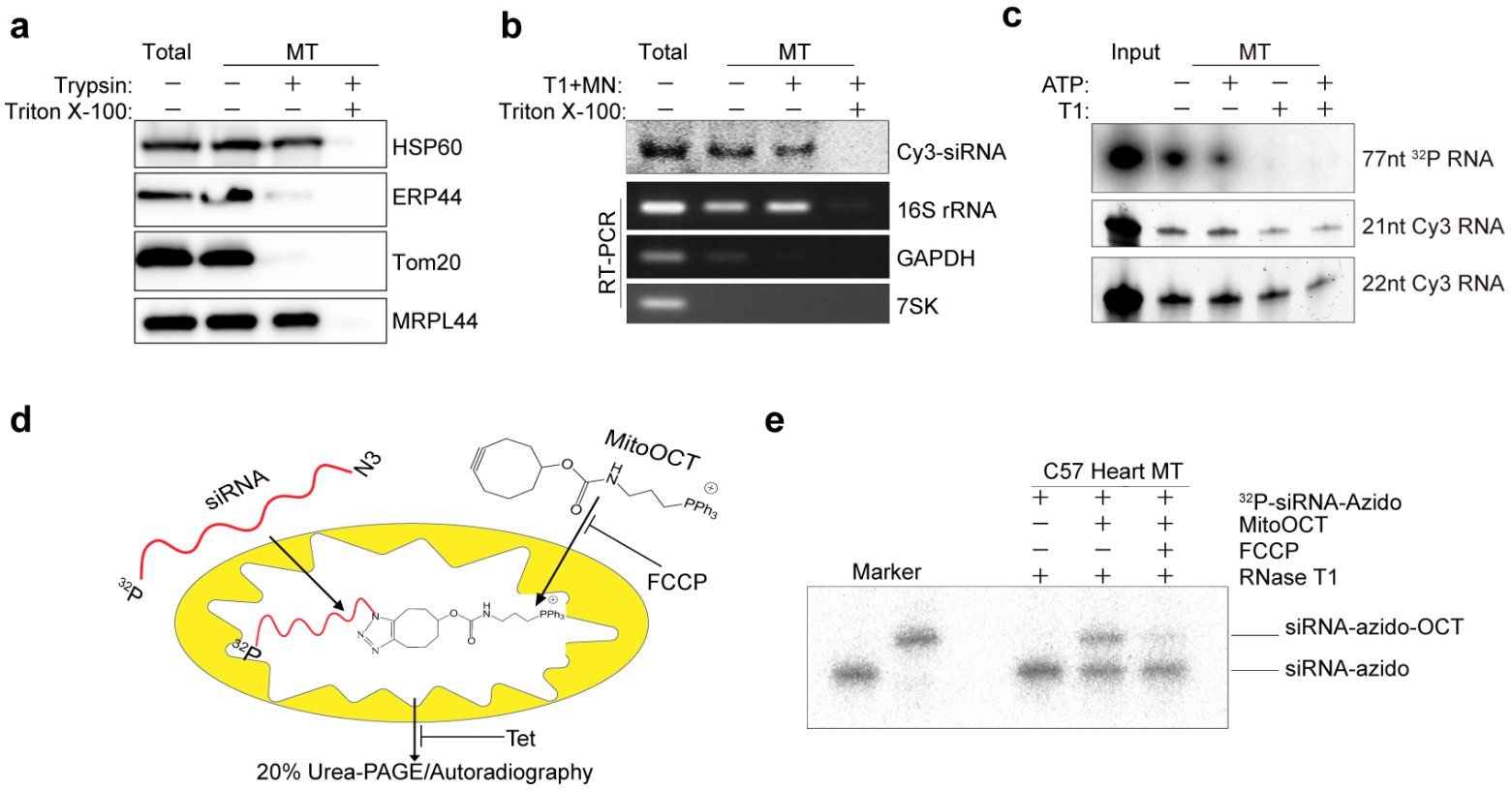
a
Total
MT
Trypsin:
Triton X-100:
HSP60
ERP44
Tom20
MRPL44
b
Total
MT
T1+MN:
Triton X-100:
Cy3-siRNA
16S rRNA
GAPDH
7SK
RT-PCR
c
Input
MT
ATP:
T1:
77nt 32P RNA
21nt Cy3 RNA
22nt Cy3 RNA
d
siRNA
N3
32P
MitoOCT
PPh3
FCCP
Tet
20% Urea-PAGE/Autoradiography
e
C57 Heart MT
32P-siRNA-Azido
MitoOCT
FCCP
RNase T1
Marker
siRNA-azido-OCT
siRNA-azido

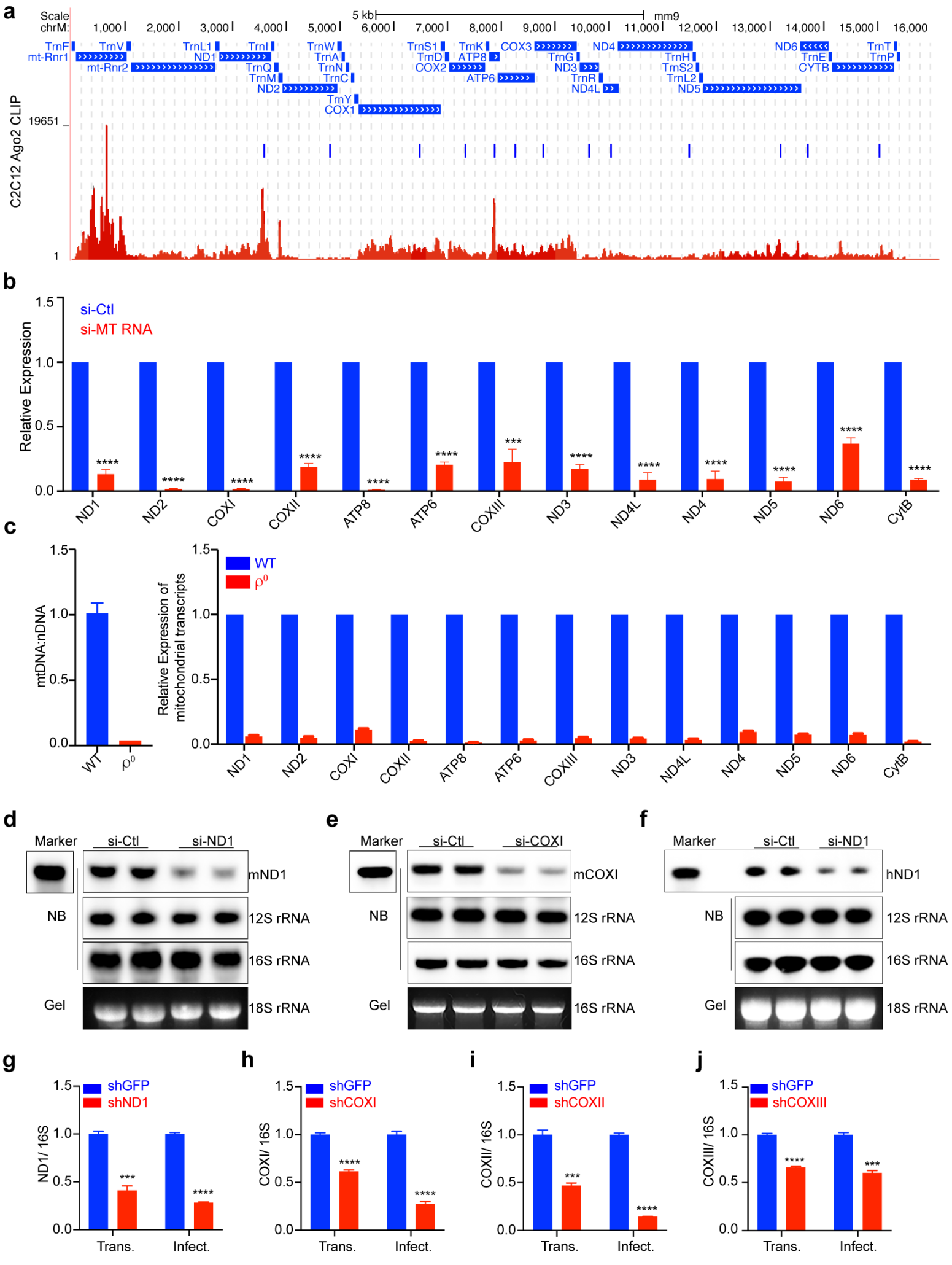
a
Scale
chrM:
5 kb
mm9
1,000
2,000
3,000
4,000
5,000
6,000
7,000
8,000
9,000
10,000
11,000
12,000
13,000
14,000
15,000
16,000
TrnF
TrnV
TrnL1
TrnI
TrnW
TrnS1
TrnK
COX3
ND4
ND6
TrnT
mt-Rnr1
ND1
TrnA
TrnD
ATP8
TrnG
TrnE
TrnP
mt-Rnr2
TrnQ
TrnN
COX2
ND3
TrnH
TrnS2
CYTB
TrnM
TrnC
ATP6
TrnR
TrnL2
ND2
ND4L
ND5
TrnY
COX1
C2C12 Ago2 CLIP
19651
1
b
si-Ctl
si-MT RNA
Relative Expression
1.5
1.0
0.5
0.0
****
***
ND1
ND2
COXI
COXII
ATP8
ATP6
COXIII
ND3
ND4L
ND4
ND5
ND6
CytB
c
mtDNA:nDNA
WT
ρ0
Relative Expression of mitochondrial transcripts
d
Marker
si-Ctl
si-ND1
mND1
NB
12S rRNA
16S rRNA
Gel
18S rRNA
e
Marker
si-Ctl
si-COXI
mCOXI
NB
12S rRNA
16S rRNA
Gel
16S rRNA
f
Marker
si-Ctl
si-ND1
hND1
NB
12S rRNA
16S rRNA
Gel
18S rRNA
g
shGFP
shND1
ND1/ 16S
Trans.
Infect.
h
shGFP
shCOXI
COXI/ 16S
Trans.
Infect.
i
shGFP
shCOXII
COXII/ 16S
Trans.
Infect.
j
shGFP
shCOXIII
COXIII/ 16S
Trans.
Infect.

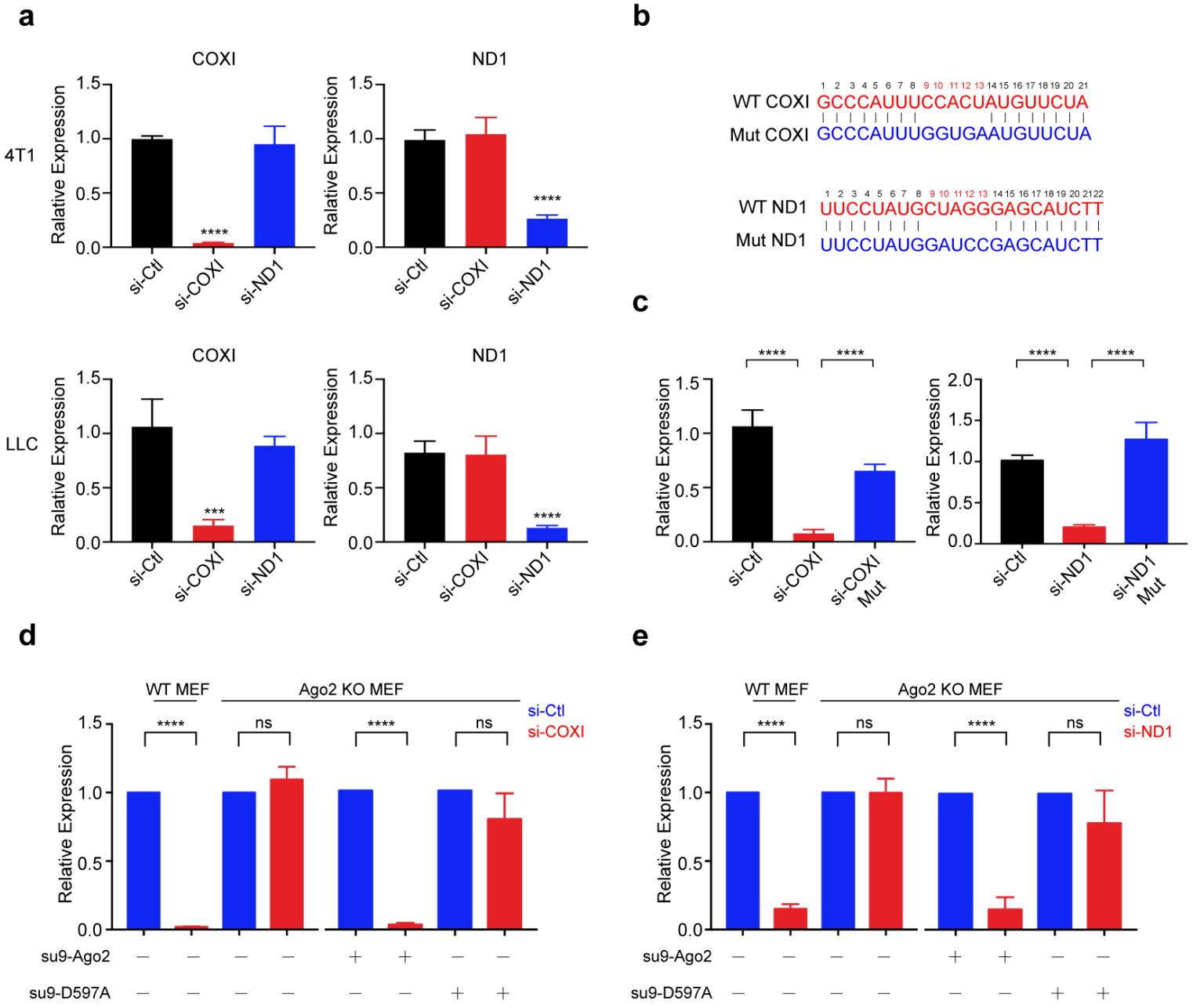
a
COXI
ND1
4T1
LLC
Ralative Expression
Relative Expression
si-Ctl
si-COXI
si-ND1
****
***
b
WT COXI GCCCAUUUCCACUAUGUUCUA
Mut COXI GCCCAUUUGGUGAAUGUUCUA
WT ND1 UUCCUAUGCUAGGGAGCAUCTT
Mut ND1 UUCCUAUGGAUCCGAGCAUCTT
c
si-COXI Mut
si-ND1 Mut
d
e
WT MEF
Ago2 KO MEF
si-Ctl
si-COXI
si-ND1
ns
su9-Ago2
su9-D597A

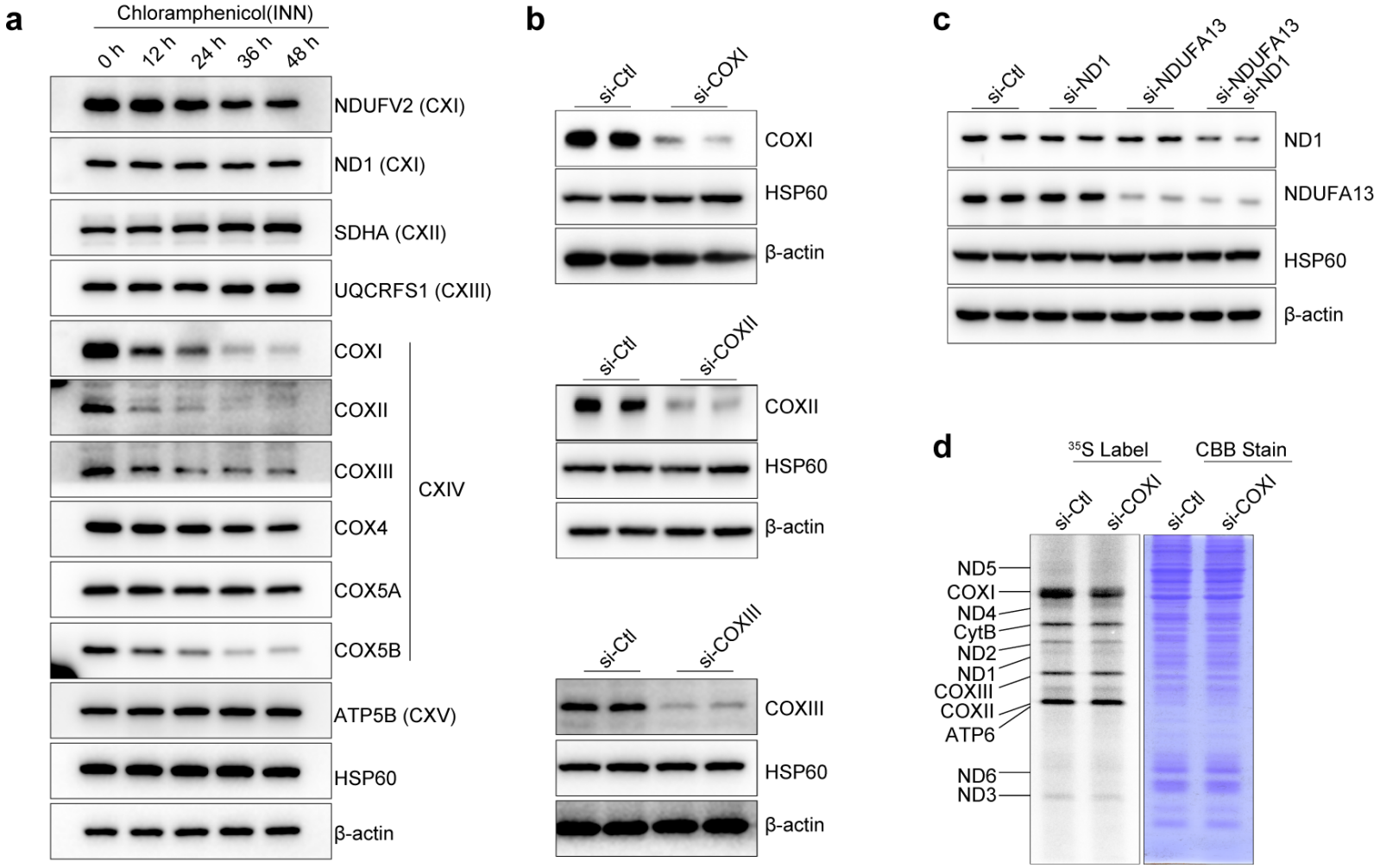
a
Chloramphenicol(INN)
0 h
12 h
24 h
36 h
48 h
NDUFV2 (CXI)
ND1 (CXI)
SDHA (CXII)
UQCRFS1 (CXIII)
COXI
COXII
COXIII
COX4
COX5A
COX5B
CXIV
ATP5B (CXV)
HSP60
β-actin
b
si-Ctl
si-COXI
COXI
HSP60
β-actin
si-Ctl
si-COXII
COXII
HSP60
β-actin
si-Ctl
si-COXIII
COXIII
HSP60
β-actin
c
si-Ctl
si-ND1
si-NDUFA13
si-NDUFA13
si-ND1
ND1
NDUFA13
HSP60
β-actin
d
35S Label
CBB Stain
si-Ctl
si-COXI
si-Ctl
si-COXI
ND5
COXI
ND4
CytB
ND2
ND1
COXIII
COXII
ATP6
ND6
ND3

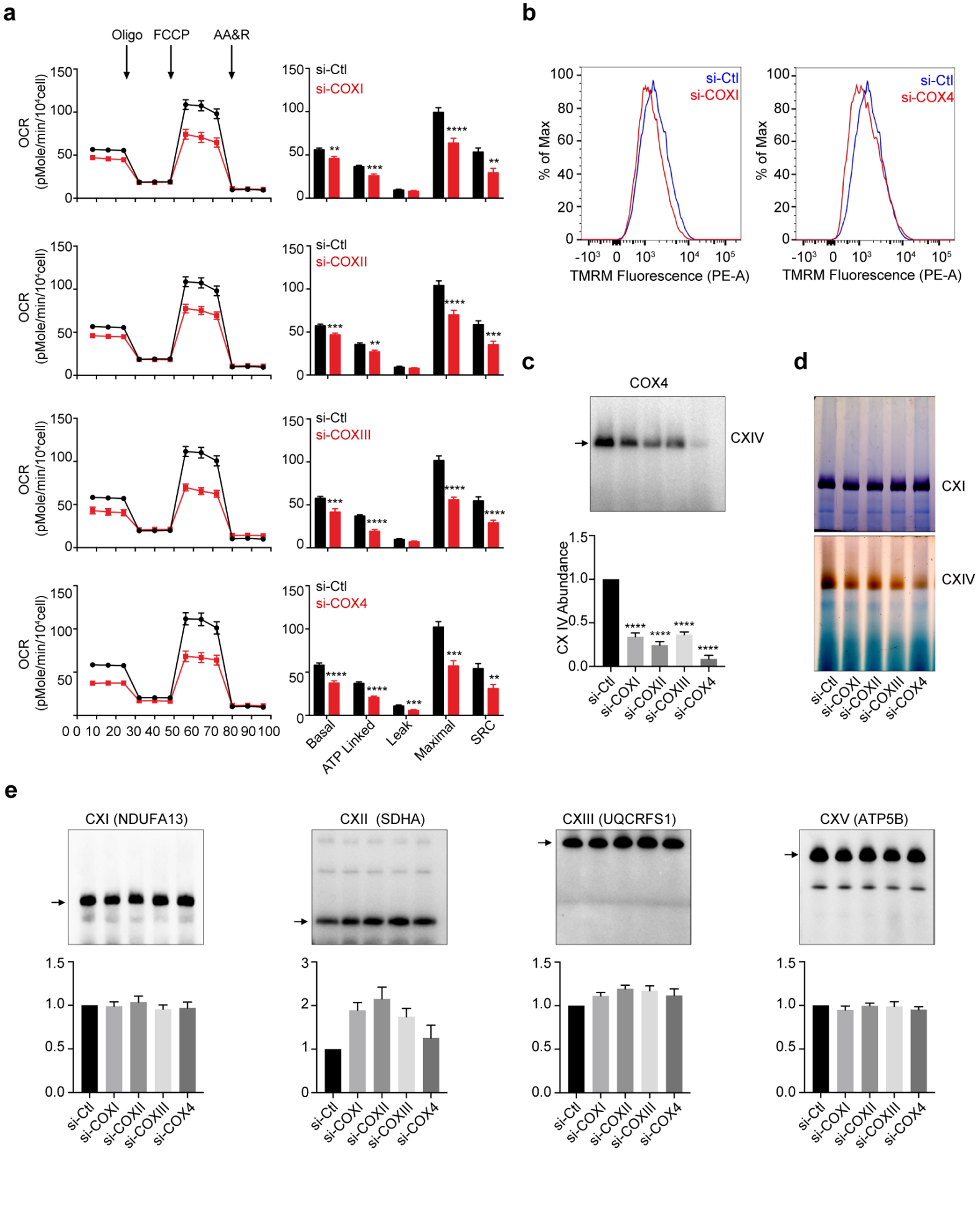
a
Oligo
FCCP
AA&R
OCR (pMole/min/10⁴cell)
si-Ctl
si-COXI
si-COXII
si-COXIII
si-COX4
Basal
ATP Linked
Leak
Maximal
SRC
b
% of Max
TMRM Fluorescence (PE-A)
c
COX4
CXIV
CX IV Abundance
d
CXI
CXIV
e
CXI (NDUFA13)
CXII (SDHA)
CXIII (UQCRFS1)
CXV (ATP5B)